IEEE Access
Multidisciplinary | Rapid Review | Open Access Journal

Received May 29, 2020, accepted June 11, 2020, date of publication July 2, 2020, date of current version July 15, 2020.

Digital Object Identifier 10.1109/ACCESS.2020.3006708

Design-Oriented Two-Stage Surrogate Modeling of Miniaturized Microstrip Circuits With Dimensionality Reduction

SLAWOMIR KOZIEL[1,2], (Senior Member, IEEE), ANNA PIETRENKO-DABROWSKA[2], (Senior Member, IEEE), AND MU'ATH AL-HASAN[3], (Senior Member, IEEE)

[1]Engineering Optimization and Modeling Center, Department of Technology, Reykjavik University, 101 Reykjavik, Iceland
[2]Faculty of Electronics, Telecommunications and Informatics, Gdansk University of Technology, 80-233 Gdansk, Poland
[3]Networks and Communication Engineering Department, Al Ain University, Abu Dhabi, United Arab Emirates

Corresponding author: Anna Pietrenko-Dabrowska (anna.dabrowska@pg.edu.pl)

This work was supported in part by the Icelandic Centre for Research (RANNIS) under Grant 206606051, in part by the National Science Centre of Poland under Grant 2018/31/B/ST7/02369, and in part by the Abu-Dhabi Department of Education and Knowledge (ADEK) Award for Research Excellence, in 2019, under Grant AARE19-245.

ABSTRACT Contemporary microwave design heavily relies on full-wave electromagnetic (EM) simulation tools. This is especially the case for miniaturized devices where EM cross-coupling effects cannot be adequately accounted for using equivalent network models. Unfortunately, EM analysis incurs considerable computational expenses, which becomes a bottleneck whenever multiple evaluations are required. Common simulation-based design tasks include parametric optimization and uncertainty quantification. These can be accelerated using fast replacement models, among which the data-driven surrogates are the most popular. Notwithstanding, a construction of approximation models for microwave components is hindered by the dimensionality issues as well as high nonlinearity of system characteristics. A partial alleviation of the mentioned difficulties can be achieved with the recently reported performance-driven modeling methods, including the nested kriging framework. Therein, the computational benefits are obtained by appropriate confinement of the surrogate model domain, spanned by a set of pre-optimized reference designs, and by focusing on the parameter space region that contains high quality designs with respect to the considered performance figures. This paper presents a methodology that incorporates the concept of nested kriging and enhances it by explicit dimensionality reduction based on spectral decomposition of the reference design set. Extensive verification studies conducted for a compact rat-race coupler and a three-section impedance matching transformer demonstrate superiority of the presented approach over both the conventional techniques and the nested kriging in terms of modeling accuracy. Design utility of our surrogates is corroborated through application cases studies.

INDEX TERMS Microwave design, compact circuits, surrogate modeling, domain confinement, principal component analysis, dimensionality reduction.

I. INTRODUCTION

Full-wave electromagnetic (EM) analysis is one of the most important tools in the design of contemporary microwave components. As a matter of fact, EM-simulation-driven design has become imperative for a considerable number of components and circuits [1]–[4]. On the one hand, the reason is reliability: analytical or network-equivalent models are unable to describe adequately systems of increasing complexity. On the other hand, for some circuits, parameterized network models may not be available whatsoever. Miniaturized microstrip components constitute a representative class of structures for which the aforementioned issues are especially pertinent. This is primarily due to considerable EM-cross couplings present in tightly arranged layouts of compact circuits, being a result of transmission line (TL)

The associate editor coordinating the review of this manuscript and approving it for publication was Luca Cassano.

folding [5], the employment of compact microwave resonant cells (CMRCs) [6], or multi-layer implementation (e.g., LTCC circuits [7], [8]).

Perhaps the most annoying inconvenience of EM-driven design is its high computational cost, which manifests itself especially in tasks that require a large number of system simulations. These include parametric optimization (also referred to as design closure) [9], multi-objective design [10], global optimization [11], as well as uncertainty quantification (statistical analysis [12], tolerance-aware design [13]). High cost often prompts the researchers to employ simplified design procedures, largely based on parameter sweeping, or to consider special cases (e.g., worst-case analysis instead of proper statistical analysis [14]), which are manageable in terms of the entailed computational expenses but grossly inaccurate. Apart from strictly algorithmic methods (e.g., gradient-based procedures with sparse sensitivity updates [15], [16]), fast surrogate models offer a way of expediting simulation-based design procedures [17]–[19]. A number of surrogate-assisted methods have been developed for local tuning purposes, where the model is only constructed along the optimization path and enhanced using the EM-simulation data acquired on the way [20]–[26]. A sufficient generalization capability of such models may be ensured by rendering them based on underlying lower-fidelity models (e.g., network equivalents) [20]. Space mapping [17] is probably the best know technique of this kind in high-frequency electronics, whereas others include various response correction techniques [23], [24], and the feature-based technology [27]. For global optimization, a popular approach is an iterative construction of the surrogate involving sequential sampling methods [28], e.g., efficient global optimization (EGO) methods [29], machine learning techniques [30], or surrogate-assisted population-based metaheuristics [31], [32].

Owing to their attractive features (versatility and easy access through various third-party toolboxes, e.g., [33], [34]), data-driven models constitute the most popular class of surrogates. Furthermore, as approximation models are exclusively based on sampled high-fidelity model data, it is straightforward to apply them in different engineering disciplines. Among many available modeling methods, the following ones are particularly popular: polynomial regression [35], artificial neural networks [36], radial basis function interpolation [37], kriging [38], support-vector regression [39], [40], polynomial chaos expansion [41]–[43], and, recently, PC kriging [44]. Unfortunately, data-driven surrogates exhibit an important disadvantage, which is a rapid increase of the number of training data samples required to ensure usable accuracy of the model as a function of the number of independent parameters and their ranges (a so-called curse of dimensionality). In the case of microwave components, additional challenge is high nonlinearity of the system responses as well as the necessity of modeling several characteristics simultaneously over broad frequency spectrum. In some cases, these issues can be addressed to a certain extent using techniques such as high-dimensional model representation (HDMR) [45], and orthogonal matching pursuit (OMP) [46]. Another option is the employment of variable-fidelity models (e.g., co-kriging [47], two-stage Gaussian process regression [48], or Bayesian model fusion [49]).

Recently, an alternative way of alleviating the difficulties pertinent to parameter ranges and dimensionality has been proposed through domain confinement [50]. The performance-driven modeling methods [50]–[53] explore the fact that the parameter sets being optimum with respect to the performance specifications pertinent to a design task at hand normally occupy small regions of the traditional box-constrained parameter spaces. This is due to considerable correlations between the parameters that need to be tuned in a synchronized manner when, for example, re-designing a device for different operating frequency, bandwidth, or different substrate parameters [51]. From the point of view of design utility, allocating training samples outside such high-quality regions would be a waste of computational resources. Based on this idea, surrogate modeling by domain confinement has been proposed in [50], where the approximation of the optimum design regions is obtained using a set of pre-optimized reference points. This initial method was only capable of handling one or two figures of interest and did not provide mechanisms for uniform data sampling. The nested kriging framework presented in [52] effectively resolved these issues by defining the surrogate model domain using the first-level model acting on the objective space of the component under considerations. Performance-driven modeling methods [50]–[53] have been shown superior over conventional techniques by rendering reliable models at low computational costs and alleviating the issue of dimensionality and parameter ranges.

Although nested kriging brings in some important benefits, among others, a simple procedure for uniform design of experiments and easy surrogate model optimization [52], the model domain dimensionality is intact as compared to the original parameter space. This has a negative effect on the model scalability but also predictive power for higher-dimensional problems (e.g., multi-section CMRC-based compact circuits [53]). In this paper, the nested kriging framework [52] is enhanced by explicit reduction of the model domain dimensionality. This is implemented at the level of orthogonal extension of the objective space image through the first-level model, which, in [52] has been carried out using the entire set of normal vectors. In the presented approach, it is realized using only the most dominant directions extracted from the principal components of the reference design set. Comprehensive numerical validation conducted for a miniaturized rat-race coupler and a compact three-section impedance matching transformer indicate that the proposed modeling methods leads to a further improvement of the surrogate predictive power (as compared to the nested kriging framework). At the same time, the models retain their design utility, which is corroborated by the application case studies.

II. METHODOLOGY: PERFORMANCE-DRIVEN MODELING WITH DIMENSIONALITY REDUCTION

The purpose of this section is to formulate the modelling methodology discussed in this work. One of its components is nested kriging [52], the recent performance-driven approach, in which the domain of the surrogate model is confined to the region containing high-quality designs (w.r.t. the selected figures of interest). Implementation-wise, the domain is determined using the so-called first-level model identified using the set of pre-optimized reference designs. The major enhancement introduced in this work is that the orthogonal extension of the objective space image through the first-level model is only conducted along a small subset of normal vectors calculated based on the principal components of the reference set. This allows for explicit reduction of the model domain and is in contrast to the nested kriging framework where the extension was conducted using all normal vectors. As demonstrated in Section III, the result is further improvement of the predictive power of the surrogate (as compared to nested kriging) and enhanced model scalability.

A. FUNDAMENTAL COMPONENTS OF MODELLING PROCESS

The modelling process is conducted with respect to the adjustable parameters of the structure at hand, denoted as $\boldsymbol{x} = [x_1 \ldots x_n]^T$. The standard (box constrained) parameter space X is defined using the lower and upper bounds on these parameters, $\boldsymbol{l} = [l_1 \ldots, l_n]^T$ and $\boldsymbol{u} = [u_1 \ldots, u_n]^T$, so that $x_k \in [l_k u_k]$ for $k = 1, \ldots, n$. The modeling process also assumed a certain number of figures of interest, denoted as $\boldsymbol{f} = [f_1 \ldots f_N]^T$, which form the objective space F. The objective space is delimited using the ranges of interest, $f_{k.\min}$ and $f_{k.\max}$, so that $f_{k.\min} \leq f_k \leq f_{k.\max}$, for $k = 1, \ldots, N$. Some examples of the figures of interest include an operating frequency of the circuit, power split ratio (in the case of couplers), fractional bandwidth (e.g., in the case of filters), etc. The performance figures may be also related to material parameters, e.g., the height and relative permittivity of a dielectric substrate used to implement the structure on.

The ranges $f_{k.\min}$ and $f_{k.\max}$ define the region of validity of the surrogate model that is to be rendered, i.e., we are interested in constructing the model that will be an accurate representation of the circuit in the parameter space areas that contains designs that are optimum or nearly optimum for all $\boldsymbol{f} \in F$. The design optimality is understood as follows. We define a scalar merit function $U(\boldsymbol{x}, \boldsymbol{f})$, which assesses the quality of the design represented by the parameter vector $\boldsymbol{x}$ in regards to the objective vector $\boldsymbol{f}$. Minimizing this function yields the design $\boldsymbol{x}^*$ that is optimum with respect to $\boldsymbol{f}$ as

$$\boldsymbol{x}^* = U_F(\boldsymbol{f}) = \arg\min_{\boldsymbol{x}} U(\boldsymbol{x}, \boldsymbol{f}) \tag{1}$$

The set of all designs $U_F(\boldsymbol{f})$, denoted as $U_F(F) = \{U_F(\boldsymbol{f}) : \boldsymbol{f} \in F\}$ form a subset of the parameter space X, which is, in general an N-dimensional object (e.g., a surface in the case of two-objective space F).

The following example illustrates the aforementioned concepts. Let us consider a microwave coupler that is supposed to operate at a frequency f_0. The optimum design is understood in the sense of maximizing the bandwidth B (symmetric w.r.t. f_0); at the same time, the power split at f_0, $|S_{21}| - |S_{31}|$ [dB], should attain the target value K_P. Given these specifications, the figures of interest, according to the notation introduced earlier, would be $f_1 = f_0$ and $f_2 = K_P$, whereas the cost function U may be defined as follows

$$U(\boldsymbol{x}, \boldsymbol{f}) = -2\min\{f_{B2}(\boldsymbol{x}) - f_0, f_0 - f_{B2}(\boldsymbol{x})\} + \beta\,[K_P - [|S_{21}(\boldsymbol{x}, f_0)| - |S_{31}(\boldsymbol{x}, f_0)|]]^2 \tag{2}$$

In (2), the frequencies f_{B1} and f_{B2} mark the lower and the upper edge of the -20 dB bandwidth, which is understood here as the range of frequencies where $\max\{|S_{11}(\boldsymbol{x})|, |S_{41}(\boldsymbol{x})|\} \leq -20$ dB. The function U also contains a penalty term. The latter serves as a regularization factor enforcing the condition $K_P = |S_{21}| - |S_{31}|$ at f_0 (here, β is a penalty coefficient).

As mentioned before, within the performance-driven modeling methods [50]–[53], the modeling process is restricted to the vicinity of the optimum design set $U_F(F)$. A particular implementation of this restriction is method-dependent but in all cases, the region $U_F(F)$ is approximated using a set of reference designs $\boldsymbol{x}^{(j)} = [x_1^{(j)} \ldots x_n^{(j)}]^T j = 1, \ldots, p$, which are obtained as $U_F(\boldsymbol{f}^{(j)})$, with $\boldsymbol{f}^{(j)} = [f_1^{(j)} \ldots f_N^{(j)}]$ being the target vectors allocated within the objective space F. The origin of the reference points may be twofold: (i) designs rendered specifically for the sake of constructing the surrogate model, and (ii) designs available as a result of prior optimization of a microwave structure at hand for various performance specifications.

Spectral decomposition of the reference design set can be used to yield important insight into correlations between the design objective and the optimum parameter sets. We will utilize this information later (Section II.*B*) in the definition of the surrogate model domain. Let

$$\boldsymbol{x}_m = \frac{1}{p}\sum_{k=1}^{p} \boldsymbol{x}^{(k)} \tag{3}$$

be a reference design set center. We define the covariance matrix $\boldsymbol{S}_p$ of $\{\boldsymbol{x}^{(k)}\}$ as

$$\boldsymbol{S}_p = \frac{1}{p-1}\sum_{k=1}^{p} (\boldsymbol{x}^{(k)} - \boldsymbol{x}_m)(\boldsymbol{x}^{(k)} - \boldsymbol{x}_m)^T \tag{4}$$

Let $\boldsymbol{a}_k$, $k = 1, \ldots, n$ be the eigenvectors of $\boldsymbol{S}_p$, and λ_k be the corresponding eigenvalues [54]. Without loss of generality, we can assume that the eigenvalues are arranged in a descending order, i.e., we have $\lambda_1 \geq \lambda_2 \geq \ldots \geq \lambda_n \geq 0$. The eigenvectors $\boldsymbol{a}_k$ are the principal components of the reference design set and they establish the directions of the most important correlations between the structure parameters at the locations of the optimum designs within the objective space F. The eigenvalues λ_k represent the variance of the

reference set in the eigenspace. Using these, we also define the matrices

$$\boldsymbol{A}_k = [\boldsymbol{a}_1 \ \ldots \ \boldsymbol{a}_k] \tag{5}$$

which contain the first k eigenvectors as columns. The matrix constructed using all eigenvectors will be denoted as $\boldsymbol{A} = \boldsymbol{A}_n$.

B. SURROGATE MODEL DOMAIN DEFINITION: FIRST-LEVEL MODEL AND ORTHOGONAL EXTENSION

The basis for constructing the surrogate model domain is the initial step of the procedure employed by the nested kriging framework [52], i.e., the first-level surrogate $\boldsymbol{s}_I(\boldsymbol{f}) : F \rightarrow X$, rendered using the set of reference points and the associated objective vectors $\{\boldsymbol{f}^{(j)}, \boldsymbol{x}^{(j)}\}, j = 1, \ldots, p$. The model itself is a kriging interpolation surrogate, and it is, in fact, an inverse model because of mapping the figures of interest (space F) into the parameter space X of the structure at hand.

The initial approximation of the optimum design set $U_F(F)$ is obtained as the image of the objective space through the first-level model, i.e., $\boldsymbol{s}_I(F)$. The two sets agree perfectly for all $\boldsymbol{f}^{(j)}$ associated with the reference designs. Notwithstanding, as the number of reference designs is normally small, $\boldsymbol{s}_I(F)$ generally does not coincide with $U_F(F)$. In the nested kriging framework, these discrepancies are accommodated by extending $\boldsymbol{s}_I(F)$ in all directions $\{\boldsymbol{v}_n^{(k)}(\boldsymbol{f})\}, k = 1, \ldots, n-N$, that are normal to $\boldsymbol{s}_I(F)$ at $\boldsymbol{f} \in F$ [52]. The scope of extension is determined by a so-called thickness coefficient D. The rule of thumb is to ensure that the lateral size of the domain is five to ten percent of the tangential size (the latter can be inferred from the span of the reference designs), which normally allows for the majority of $U_F(F)$ to become a subset of the model domain. It should be noted that within the aforementioned setup, the dimensionality of the domain is the same as the dimensionality of the parameter space X.

The purpose of this work is to employ the spectral analysis of the reference set (cf. (3)-(5)) in order to provide explicit reduction of the domain dimensionality. Towards this end, the orthogonal extension of the first-level model image will be conducted only with respect to a few normal vectors corresponding to the most significant directions as determined by the eigenvectors $\boldsymbol{a}_k$ (cf. Section II.A). We will denote the number of such directions as $K \leq n$. It should be observed that K has to be larger than the dimensionality of the objective space N to ensure that the extension is non-trivial.

Having K, the task is to obtain the extension vectors using the eigenvectors $\boldsymbol{a}_k$, $k = 1, \ldots, K$. To this end, we denote as $\boldsymbol{t}_j(\boldsymbol{f})$, $j = 1, \ldots, N$, the vectors tangent to $\boldsymbol{s}_I(F)$ at the objective vector $\boldsymbol{f}$. The first step is to represent $\{\boldsymbol{t}_j(\boldsymbol{f})\}_{j=1,\ldots,N}$ with respect to the eigenvectors $\{\boldsymbol{a}_k\}_{k=1,\ldots,K}$, which can be obtained as

$$\left[\bar{\boldsymbol{t}}_1(\boldsymbol{f}) \ \ldots \ \bar{\boldsymbol{t}}_N(\boldsymbol{f})\right] = \boldsymbol{A}_K^T \left[\boldsymbol{t}_1(\boldsymbol{f}) \ \ldots \ \boldsymbol{t}_N(\boldsymbol{f})\right] \tag{6}$$

In (6), the matrix $\boldsymbol{A}_K$ is defined according to (5). The size of vectors $\bar{\boldsymbol{t}}_j(\boldsymbol{f})$ is $K \times 1$, in other words, we want to restrict our considerations (in particular, the surrogate model domain) to the K-dimensional subspace spanned by the columns of $\boldsymbol{A}_K$.

The next step is to find a set of vectors normal to $\boldsymbol{s}_I(F)$ but within the subspace spanned by $\boldsymbol{A}_K$. Towards this end, consider the matrix $\boldsymbol{T}(\boldsymbol{f})$

$$\boldsymbol{T}(\boldsymbol{f}) = \left[\bar{\boldsymbol{t}}_1(\boldsymbol{f}) \ \ldots \ \bar{\boldsymbol{t}}_N(\boldsymbol{f}) \ \boldsymbol{e}_{N+1} \ \boldsymbol{e}_{N+2} \ \ldots \ \boldsymbol{e}_K\right] \tag{7}$$

which is a complement of $\left[\bar{\boldsymbol{t}}_1(\boldsymbol{f}) \ \ldots \ \bar{\boldsymbol{t}}_N(\boldsymbol{f})\right]$ to a square $K \times K$ matrix, where $\boldsymbol{e}_j = [0 \ \ldots \ 0 \ 1 \ 0 \ \ldots \ 0]^T$ with 1 at the jth position. At this point, we apply a Gram-Schmidt procedure [55] to $\boldsymbol{T}(\boldsymbol{f})$ in order to render an orthonormal basis of K vectors $\boldsymbol{T}_{GS}$ of the form

$$\boldsymbol{T}_{GS}(\boldsymbol{f}) = \left[\tilde{\boldsymbol{t}}_1(\boldsymbol{f}) \ \ldots \ \tilde{\boldsymbol{t}}_N(\boldsymbol{f}) \ \boldsymbol{w}_1(\boldsymbol{f}) \ \ldots \ \boldsymbol{w}_{K-N}(\boldsymbol{f})\right] \tag{8}$$

The matrix (8) has two parts, the second consisting of the vectors $\boldsymbol{w}_j(\boldsymbol{f})$, $j = 1, \ldots, K-N$, which will be used to carry out the orthogonal extension of $\boldsymbol{s}_I(F)$. It can be observed that because the tangent vectors $\boldsymbol{t}_j(\boldsymbol{f})$ are generally well aligned with the eigenvectors $\boldsymbol{a}_j$, $j = 1, \ldots, N$, the vectors $\tilde{\boldsymbol{t}}_j(\boldsymbol{f})$ are close to $\bar{\boldsymbol{t}}_j(\boldsymbol{f})$. Also, it has to be emphasized that the vectors $\boldsymbol{w}_j(\boldsymbol{f})$ are functions of the objective vector $\boldsymbol{f}$, so that they have to be computed separately for each $\boldsymbol{f} \in F$. Selecting an appropriate dimensionality K is an important consideration, which can be facilitated by means of analyzing the eigenvalues λ_k. Typically, $K = N + 1$ or $N + 2$ is sufficient. An extended discussion of this issue will be provided in Section III.

The final step is to define the surrogate model domain itself, here, denoted at X_S, which involves both the first-level model $\boldsymbol{s}_I()$ and the vectors $\boldsymbol{w}_j$. We have

$$X_S = \left\{ \begin{array}{c} \boldsymbol{x} = \boldsymbol{s}_I(\boldsymbol{f}) + T \sum_{k=1}^{K-N} \alpha_k \boldsymbol{w}_n^{(k)}(\boldsymbol{f}) : \boldsymbol{f} \in F, \\ -1 \leq \alpha_k \leq 1, \ k = 1, \ldots, n-N \end{array} \right\} \tag{9}$$

It should be noted that X_S consists of all points of the form $\boldsymbol{x} = \boldsymbol{s}_I(\boldsymbol{f}) + T \sum_{k=1}^{K-N} \alpha_k \boldsymbol{w}_n^{(k)}(\boldsymbol{f})$, which are generated for all $\boldsymbol{f} \in F$ and all combinations of coefficients α_k with $-1 \leq \alpha_k \leq 1$ for $k = 1, \ldots, K-N$. The parameter T used in (9) plays a role similar to that of the thickness parameter D of nested kriging. In general, it is possible to employ separate coefficients for all expansion directions (i.e., T_k, $k = 1, \ldots, K-N$, instead of a common T), which would allow to distinguish between the relative importance of particular directions (e.g., based on the corresponding eigenvalues). However, in the verification experiments presented in Section III, a joint parameter T is utilized for the sake of simplicity. It is set to a few percent of the reference set size towards the most dominant eigenvector $\boldsymbol{a}_1$; furthermore, it is adjusted to account for the relationships between the eigenvalues λ_k.

The surrogate model domain dimensionality is controlled by the parameter K (the number of principal components $\boldsymbol{a}_k$ used in the domain definition). In particular, setting $K = n$ (the maximum number of components, equal to the dimensionality of the parameter space) is almost equivalent to going back to the original nested kriging. As a matter of fact, the latter is used later in the work (Section III) as one of the benchmark techniques, in order to demonstrate the benefits of dimensionality reduction.

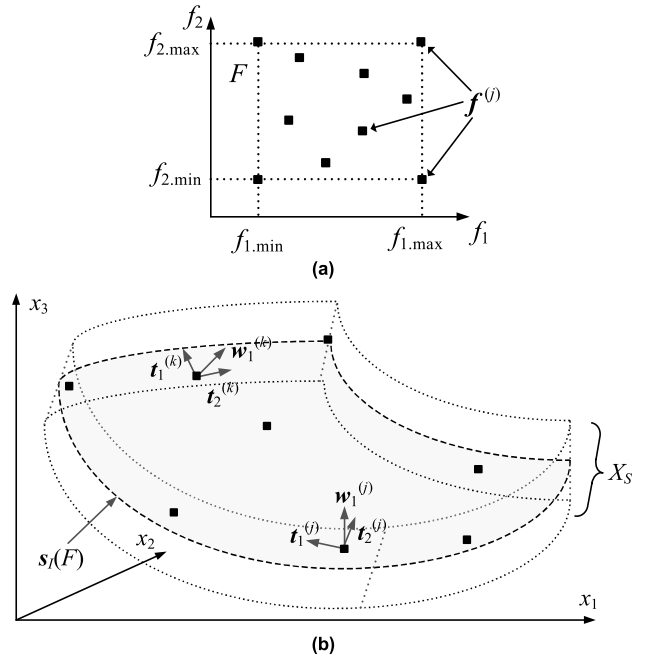

FIGURE 1. Performance-driven modeling with explicit dimensionality reduction: basic components. For clarity, the concepts are shown using a two-dimensional objective space and the three-dimensional parameter space: (a) objective space F, (b) parameter space X, the reference designs, the optimum design set $U_F(F)$, and the first-level model image $s_I(F)$ (gray-shaded surface). The picture also shows two exemplary points $s_I(f)$ along with their corresponding tangent vectors t_1 and t_2, and the normal vector w_1 obtained as in (8). In general, the target dimensionality K of the domain X_S is smaller than the dimensionality n of X. However, as shown in the picture, $K = n$ to enable a graphical representation.

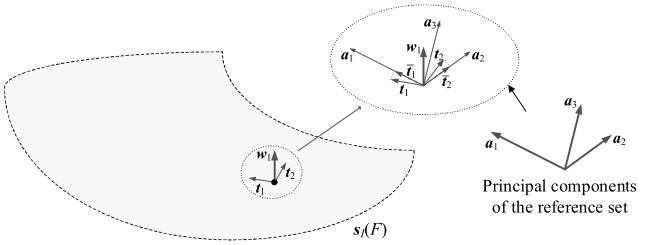

FIGURE 2. Construction of the extension basis $\{w_i(f)\}$ of (8) – graphical illustration. The visualization is provided assuming three-dimensional parameter space and two-dimensional objective space (cf. Fig. 1), as well $K = n$ (the number of domain-defining principal components equal to the dimensionality of the parameter space) to make the illustration possible. Shown are: the set $s_I(F)$ along with a selected reference design, its corresponding tangent vectors $\{t_j\}$, and zoom onto the construction procedure shown in the inset. The projected vectors $\bar{t}_j(f)$ are obtained as in (6). The extension vectors w_i are obtained using the Gram-Schmidt procedure (cf. (7) and (8)).

The fundamental components of the presented modeling procedure have been illustrated in Fig. 1. A graphical illustration of constructing the extension vectors $\{w_i(f)\}$ can be found in Fig. 2.

C. CONSTRUCTING THE SURROGATE. DOMAIN SAMPLING AND SURROGATE OPTIMIZATION

Having the domain X_S defined as in Section II.C, the actual surrogate model $s(x)$ is constructed in a conventional manner,

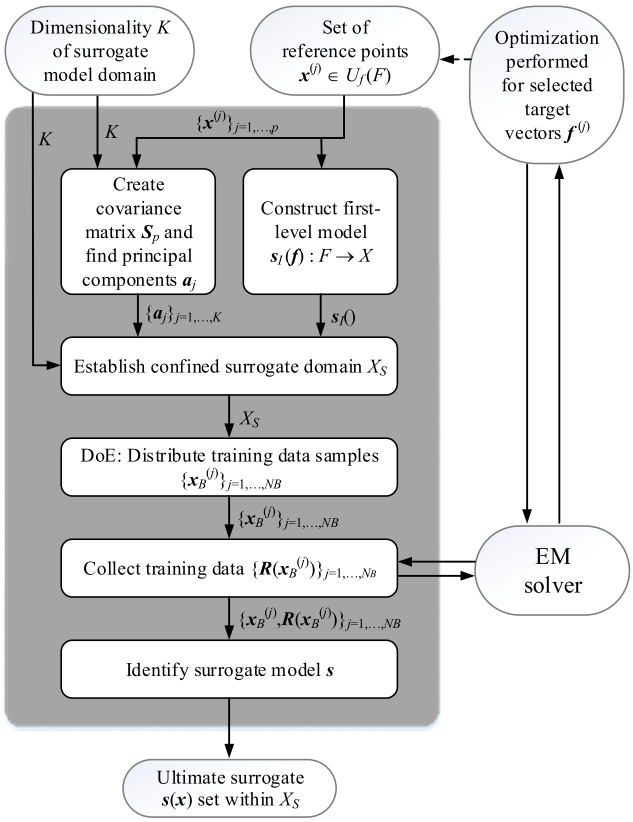

FIGURE 3. Performance-driven modeling with dimensionality reduction: flow diagram.

here, using kriging interpolation [56]. The training data pairs will be denoted as $\{x_B^{(k)}, R(x_B^{(k)})\}_{k=1,...,NB}$, where $x_B^{(k)} \in X_S$ are the samples, whereas $R(x_B^{(k)})$ are the evaluations of the full-wave EM-simulation model of the structure being modeled. The flow diagram of the modeling process has been shown in Fig. 3.

There are two direct benefits of constraining the surrogate model domain. On the one hand, because the volume of X_S is significantly smaller than that of the original parameter space X, the modeling accuracy is expected to be considerably improved (assuming the same training data set sizes) [52]. On the other hand, the accuracy improvement is achieved without formally restricting neither the ranges of geometry nor operating parameters of the structure. These advantages are even more noticeable in higher-dimensional cases where conventional modeling (i.e., within the domain X) is infeasible, whereas reliable performance-driven surrogates can still be rendered. Reduction of the domain dimensionality as proposed in this work is a supplementary advantage. As demonstrated in Section III, it leads to a further improvement of the model predictive power but also modeling error scalability with respect to the training data set size.

A few comments should be made at this point about the design of experiments (DoE). Space-filling DoE in X_S is not straightforward due to the complex geometry of the domain.

In this work, we follow the approach presented in [52], directly based on the domain definition, and adopted for our needs. More specifically, we employ a surjective mapping between the unit interval $[0, 1]^K$ and the domain X_S. Let us assume that $\{z^{(k)}\}$, $k = 1, \ldots, N_B$, is a training data set, with the samples uniformly distributed in $[0, 1]^K$ by means of, e.g., Latin Hypercube Sampling [57]. A transformation $H : [0, 1]^K \rightarrow X_S$ is defined as

$$\boldsymbol{x} = H(\boldsymbol{z}) = H([z_1 \ \ldots \ z_n]^T) = \boldsymbol{s}_I\left(\boldsymbol{f}_z\right) + T\sum_{k=1}^{K-N}(-1 + 2z_{N+k})\boldsymbol{w}_n^{(k)}(\boldsymbol{f}_z) \quad (10)$$

in which

$$\boldsymbol{f}_z = \begin{bmatrix} f_{1.\min} + z_1(f_{1.\max} - f_{1.\min}) \\ \vdots \\ f_{N.\min} + z_N(f_{N.\max} - f_{N.\min}) \end{bmatrix} \quad (11)$$

The uniformly distributed sample set $\{\boldsymbol{x}_B^{(k)}\}$ in X_S is then obtained using the transformation H as

$$\boldsymbol{x}_B^{(k)} = H(\boldsymbol{z}^{(k)}), \quad k = 1, \ldots, N_B \quad (12)$$

It is important to mention that the sample set is uniform with respect to the objective space F, i.e., the points $\boldsymbol{f}_z(\boldsymbol{z}^{(k)})$, $k = 1, \ldots, N_B$, obtained using (11) are uniformly filling F. This means, in particular, that if f_1 represents, e.g., the operating frequency of a coupler, the sample set uniformity refers to equal representation of the coupler designs corresponding to the different operating frequencies ranging from $f_{1.\min}$ to $f_{1.\max}$.

The mapping H can also be used to facilitate applications of the surrogate model to solving design tasks such as parametric optimization. Let us consider the design problem (1) featuring the merit function U and the target vector $\boldsymbol{f}_t$. The problem can be formulated as follows

$$\boldsymbol{x}^* = \arg\min_{\boldsymbol{x}\in[0,1]^K} U(H(\boldsymbol{z}), \boldsymbol{f}_t) \quad (13)$$

and solved over the normalized interval $[0,1]^K$. The first-level surrogate $\boldsymbol{s}_I$ can be then used to identify a good initial design as (cf. [52])

$$\boldsymbol{x}^{(0)} = \boldsymbol{s}_I(\boldsymbol{f}_t) \quad (14)$$

The vector $\boldsymbol{x}^{(0)}$ is the best possible approximation of the design $\boldsymbol{x}^* = U_F(\boldsymbol{f}_t)$ one can extract from the data contained in the reference designs.

III. VERIFICATION STUDIES

The purpose of this section is to provide numerical verification of the modelling procedure presented in Section II. It is based on two miniaturized microwave components, a rat-race coupler and a three-section impedance matching transformer. For the sake of benchmarking, the section also includes comparisons with conventional modelling approaches and the nested kriging of [52]. Application case studies are also discussed in order to demonstrate the design utility of the proposed approach. Here, we assume that the designer already establishes the topology of the device at hand during the early stages of the design process and through the initial parametric studies. That includes the structure parameterization, which is therefore assumed to be fixed.

A. CASE 1: THREE-SECTION CMRC-BASED IMPEDANCE MATCHING TRANSFORMER

Consider a compact three-section 50-to-100 Ohm impedance matching transformer of [58]. The circuit geometry has been shown in Fig. 4(a). The fundamental building blocks of the transformer are compact microstrip resonant cells (CMRCs) shown in Fig. 4(b). Their purpose is to reduce the overall length of the structure as compared to the implementation based on conventional transmission lines. The circuit is implemented on RF-35 substrate ($\varepsilon_r = 3.5$, $h = 0.762$ mm, $\tan\delta = 0.018$). Its geometry is described by fifteen parameters $\boldsymbol{x} = [l_{1.1}\ l_{1.2}\ w_{1.1}\ w_{1.2}\ w_{1.0}\ l_{2.1}\ l_{2.2}\ w_{2.1}\ w_{2.2}\ w_{2.0}\ l_{3.1}\ l_{3.2}\ w_{3.1}\ w_{3.2}\ w_{3.0}]^T$. The computational model is simulated in CST Microwave Studio using its transient solver (∼280,000 mesh cells, simulation time 2.5 min). The frequency simulation range is from 0.5 GHz to 7.5 GHz.

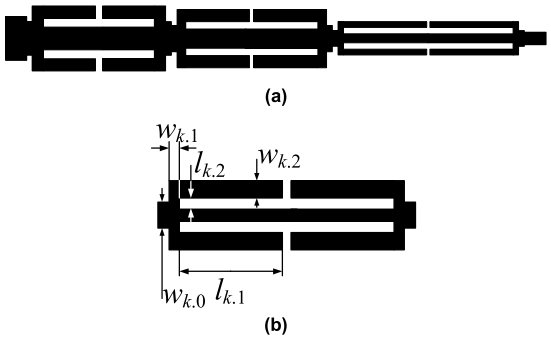

FIGURE 4. Verification case study 1: compact CMRC-based 3-section impedance matching transformer: (a) circuit topology, (b) parameterized geometry of the compact microstrip resonant cell (CMRC).

The modeling goals are the following. We aim at constructing the surrogate that is valid for the operating bands $[f_1\ f_2]$ defined by the requirement $|S_{11}| \leq -20$ dB, with 1.5 GHz $\leq f_1 \leq$ 3.5 GHz, and 4.5 GHz $\leq f_2 \leq$ 6.5 GHz. The conventional parameter space X is defined using the lower and upper bounds $\boldsymbol{l} = [2.0\ 0.15\ 0.65\ 0.35\ 0.30\ 2.70\ 0.15\ 0.44\ 0.15\ 0.30\ 3.2\ 0.15\ 0.30\ 0.15\ 0.30]^T$, and $\boldsymbol{u} = [3.4\ 0.50\ 0.80\ 0.55\ 1.90\ 4.00\ 0.50\ 0.67\ 0.50\ 1.55\ 4.5\ 0.26\ 0.46\ 0.27\ 1.75]^T$. The first-level model is constructed using nine reference points, optimized for all combinations of $f_1 \in \{1.5, 2.5, 3.5\}$ GHz and $f_2 \in \{4.5, 5.5, 6.5\}$ GHz.

The verification experiments have been set up as described below. The proposed surrogate is constructed using several training sets of sizes 50, 100, 200, 400, and 800 samples. The split sample method [56] based on 100 random test points is employed to estimate the modeling error. The assumed metric is the average value of the relative RMS error, defined as $||\boldsymbol{R}_f(\boldsymbol{x}) - \boldsymbol{R}_s(\boldsymbol{x})||/||\boldsymbol{R}_f(\boldsymbol{x})||$, where $\boldsymbol{R}_f$ and $\boldsymbol{R}_s$ stand for the EM-simulated and surrogate model outputs, respectively.

The benchmark methods include conventional kriging and radial basis function (RBF, [37]) models (both within the interval $[\boldsymbol{l}, \boldsymbol{u}]$), as well as the nested kriging model of [52] constructed for the thickness parameter $D = 0.05$. In addition to that, the proposed model was considered in several variants, corresponding to the following numbers of principal directions: $K = 3$, 4, and 5. For all cases, the extension parameter T was set to 0.25 mm, which was set up as follows. The overall span of the conventional domain X calculated as $||\boldsymbol{u} - \boldsymbol{l}||$ is about 3.5 mm, whereas the fourth eigenvalue λ_4 is about four percent of the largest one λ_1. Thus, $T = 0.25$ mm (i.e., orthogonal span of the domain X_S) corresponds to about seven percent of the overall span, which is comparable to the amount of information carried by the fourth principal component (here, for the sake of example, the second one that contributes to the orthogonal extension of $\boldsymbol{s}_I(F)$).

TABLE 1. Verification case 1: modeling results for the impedance matching transformer.

Number of training samples	Relative RMS Error					
	Conventional Models		Nested Kriging Model [52]	Proposed Model (Nested Kriging with PCA)		
	Kriging	RBF		$K = 3$	$K = 4$	$K = 5$
50	49.1 %	56.2 %	17.3 %	10.0 %	13.8 %	15.7 %
100	31.1 %	33.0 %	13.9 %	6.1 %	8.7 %	11.3 %
200	25.9 %	27.5 %	10.3 %	5.7 %	7.6 %	8.5 %
400	20.4 %	23.1 %	7.4 %	5.4 %	6.8 %	7.7 %
800	15.7 %	16.8 %	6.1 %	4.9 %	5.2 %	6.3 %

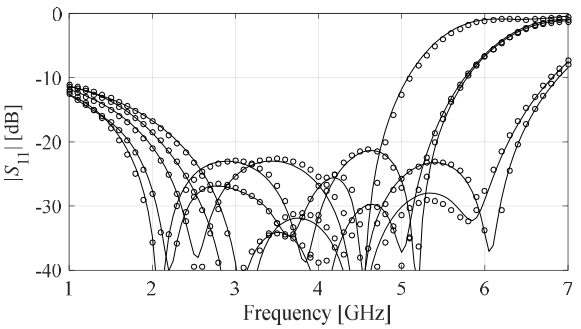

FIGURE 5. Verification case 1: reflection characteristics of the impedance matching transformer of Fig. 4(a) at the selected test designs: EM model (—), proposed surrogate set up for $K = 4$ and $N = 200$ training data samples (o).

Table 1 provides the numerical results for the proposed and the benchmark modeling techniques. The surrogate and EM-simulated transformer responses at the selected test locations have been shown in Fig. 5. The results of Table 1 clearly indicate superiority of both the nested kriging and the proposed approach over the conventional methods. Both conventional kriging and RBF surrogates exhibit poor performance even for the largest considered data sets of 800 samples. The proposed surrogate is considerably better than the nested kriging model for $K = 3$ and 4, and comparable for $K = 5$; however, for all considered values of K, it is more reliable

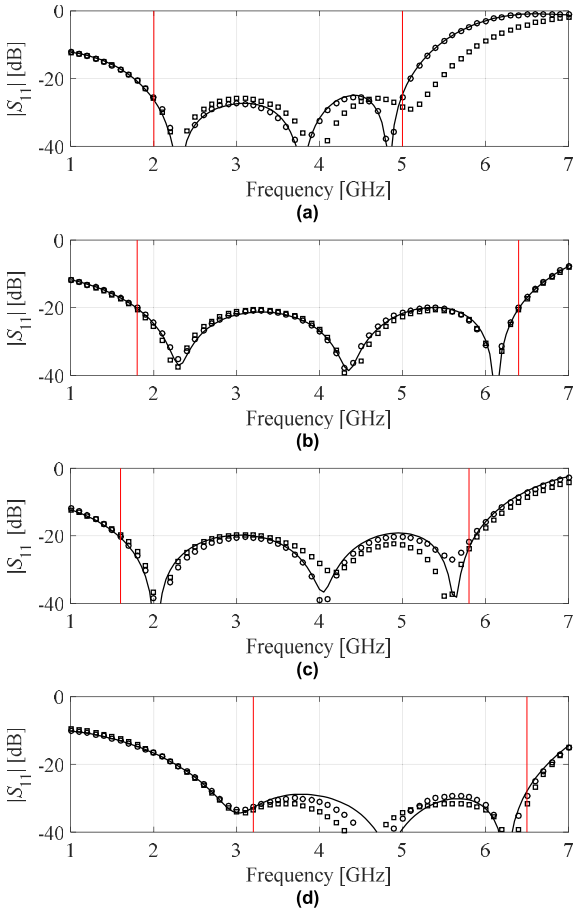

FIGURE 6. Application cases studies (design optimization) for impedance matching transformer of Fig. 4(a): proposed surrogate (o), nested kriging model [44] (□), and EM simulation at the design produced by the proposed model (—). The vertical lines denote the target operating frequency range: (a) $f_1 = 2.0$ GHz, $f_2 = 5.0$ GHz, (b) $f_1 = 1.8$ GHz, $f_2 = 6.4$ GHz, (c) $f_1 = 1.8$ GHz, $f_2 = 5.8$ GHz, (d) $f_1 = 3.2$ GHz, $f_2 = 6.5$ GHz.

for small training data set sizes of 50 to 200 samples (around twice as accurate for $K = 3$). The question arises whether going beyond $K = 4$ is justified at all. The first six normalized eigenvalues of the reference set for this problem are $\lambda_1 = 1.00$, $\lambda_2 = 0.76$, $\lambda_3 = 0.15$, $\lambda_4 = 0.041$, $\lambda_5 = 0.008$, $\lambda_6 = 0.003$. This indicates that using more than three or four eigenvectors is not necessary as the information brought by including subsequent dimensions becomes negligible.

In order to verify the design utility of the proposed modeling procedure, the model obtained with $K = 4$ and $N = 400$ has been optimized for several target bandwidths, and compared to the results obtained by means of the nested kriging model (for the same objectives). The results have been visualized in Fig. 6, clearly demonstrating that dimensionality reduction does not negatively affect the design quality. Table 2 contains the values of the geometry parameters at the optimized designs.

B. CASE 2: MINIATURIZED RAT-RACE COUPLER

The second verification case is a miniaturized microstrip rat-race coupler (RRC) [59], also implemented on

TABLE 2. Application case studies: optimization of the impedance transformer of Fig. 4(a).

Target operating conditions		Geometry parameter values [mm]														
f_1 [GHz]	f_2 [GHz]	$l_{1.1}$	$l_{1.2}$	$w_{1.1}$	$w_{1.2}$	$w_{1.0}$	$l_{2.1}$	$l_{2.2}$	$w_{2.1}$	$w_{2.2}$	$w_{2.0}$	$l_{3.1}$	$l_{3.2}$	$w_{3.1}$	$w_{3.2}$	$w_{3.0}$
2.0	5.0	3.08	0.31	0.76	0.50	1.20	3.83	0.27	0.54	0.23	0.73	4.14	0.17	0.34	0.18	1.00
1.8	6.4	2.74	0.21	0.80	0.40	0.54	3.28	0.16	0.65	0.16	0.41	3.54	0.16	0.42	0.16	0.69
1.8	5.8	3.14	0.18	0.79	0.39	0.55	3.61	0.18	0.63	0.15	0.34	3.84	0.16	0.41	0.16	1.19
3.2	6.5	2.20	0.33	0.80	0.50	0.92	3.22	0.15	0.66	0.14	0.51	3.31	0.15	0.36	0.15	0.29

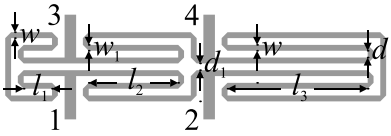

FIGURE 7. Verification case study 2: miniaturized microstrip rat-race coupler (RRC) [59].

RF-35 substrate ($\varepsilon_r = 3.5$, $h = 0.762$ mm, $\tan\delta = 0.0018$). The circuit geometry, shown in Fig. 7, is parametrized by the variable vector $\boldsymbol{x} = [l_1\ l_2\ l_3\ d\ w\ w_1]^T$; the remaining dimensions are $d_1 = d + |w - w_1|$, $d = 1.0$, $w_0 = 1.7$, and $l_0 = 15$ fixed (all in mm). The computational model is simulated in CST Microwave Studio using its frequency solver (∼120,000 mesh cells, simulation time 2.5 min) within the simulation range from 0.5 GHz to 2.5 GHz.

Here, the purpose is to construct the surrogate model covering the range of operating frequencies f_0 between 1 GHz and 2 GHz, as well as the power split ratio K_P from −6 dB to 0 dB. The optimum design of the coupler is understood in the sense of (i) maintaining the required power split at the operating frequency, i.e., $|S_{21}| - |S_{31}| = K_P$, and (ii) minimization of the matching $|S_{11}|$ and isolation $|S_{41}|$, also at f_0. The cost function quantifying the aforementioned requirements takes the form of

$$U(\boldsymbol{x},\boldsymbol{f}) = \max\{|S_{11}(\boldsymbol{x},f_0)|, |S_{41}(\boldsymbol{x},f_0)|\} + \beta\,[K_P - [|S_{21}(\boldsymbol{x},f_0)| - |S_{31}(\boldsymbol{x},f_0)|]]^2 \quad (15)$$

where the primary objective is minimization of the matching/isolation responses at f_0, whereas the penalty term is to ensure that $K_P = |S_{21}| - |S_{31}|$ at f_0 (cf. (2), Section II.A).

The reference designs are optimized for the following pairs of the operating frequency and power split ratio $\{f_0, K\}$: {1.0,0.0}, {1.0,−2.0}, {1.0,−6.0}, {1.2,−4.0}, {1.3,0.0}, {1.5,−5.0}, {1.5,−2.0}, {1.7,−6.0}, {1.7,0.0}, {1.8,−3.0}, {2.0,0.0}, {2.0,−6.0} (frequency in GHz, power split in dB). Based on these designs, the parameter space X is established and delimited by the lower bounds $\boldsymbol{l} = [2.0\ 7.0\ 12.5\ 0.2\ 0.7\ 0.2]^T$, and the upper bounds $\boldsymbol{u} = [4.5\ 12.5\ 22.0\ 0.65\ 1.5\ 0.9]^T$.

The verification experiments have been set up similarly as in Section III.A. The proposed surrogate is constructed using the training sets of sizes from 50 to 800 samples, and, in each case, for the following two domain dimensionalities, $K = 3$ and $K = 4$. Using $K = 5$ as for the previous example was not quite relevant due to the parameter space dimensionality being $n = 6$. The extension parameter T was set to 0.25 mm, based on similar considerations as presented for the previous example. The overall span of the conventional domain X, $||\boldsymbol{u} - \boldsymbol{l}||$ is about 11.3 mm, whereas already the third eigenvalue λ_3 is about three percent of the largest one λ_1. Thus, $T = 0.25$ mm (i.e., orthogonal span of the domain X_S) corresponds to less than four percent of the overall span, which is comparable to the amount of information carried by the third principal component.

The model accuracy (average relative RMS error) has been assessed using the split sample approach. The benchmark includes kriging and radial basis function (RBF) models established over the domain X, as well as the nested kriging model of [52] constructed for the thickness parameter $D = 0.05$.

TABLE 3. Verification case 2: modeling results for the rat-race coupler.

Number of training samples	Relative RMS Error				
	Conventional Models		Nested Kriging Model [52]	Proposed Model (Nested Kriging with PCA)	
	Kriging	RBF		$K = 3$	$K = 4$
50	25.7 %	28.3 %	6.9 %	5.4 %	7.1 %
100	17.9 %	19.1 %	5.7 %	3.4 %	5.4 %
200	13.5 %	13.9 %	3.8 %	3.1 %	4.1 %
400	9.9 %	10.3 %	3.5 %	2.3 %	3.4 %
800	8.0 %	8.9 %	3.1 %	1.9 %	2.9 %

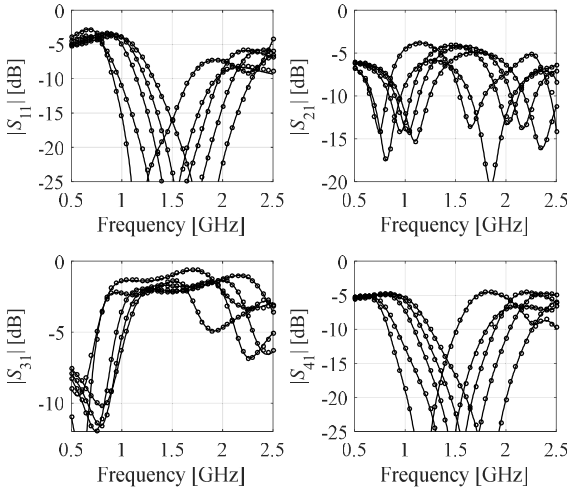

FIGURE 8. Verification case 2: responses $|S_{11}|$, $|S_{21}|$, $|S_{31}|$ and $|S_{41}|$ of the rat-race coupler of Fig. 7 at the selected test designs: EM simulated response (–), proposed surrogate set up with $K = 3$ and $N = 400$ training samples (o).

The numerical results for the proposed and the benchmark modeling techniques have been gathered in Table 3. Figure 8 visualizes the coupler characteristics for the proposed

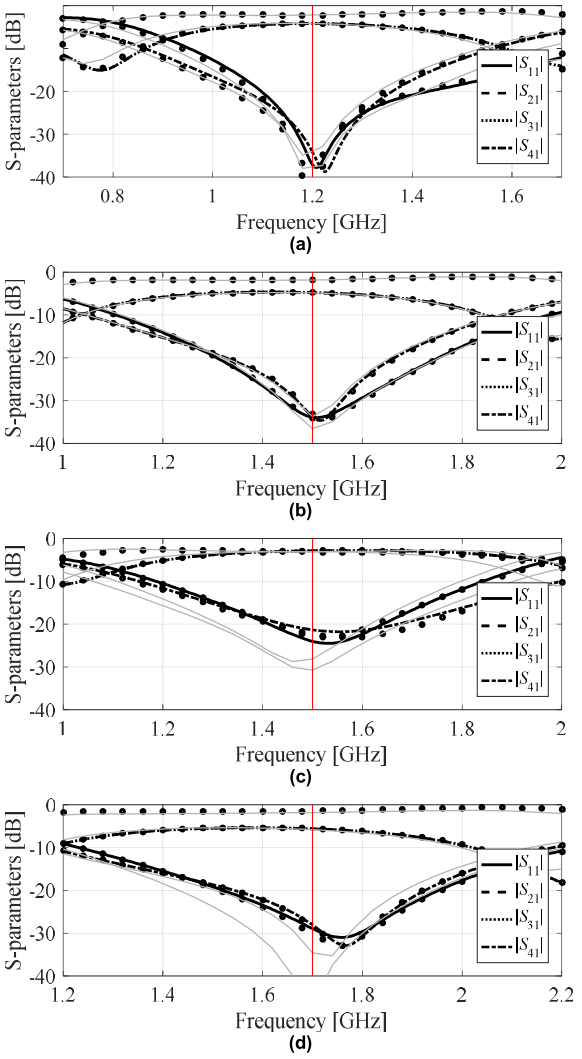

FIGURE 9. Application case studies (design optimization) for the rat-race coupler of Fig. 7: proposed surrogate (o), nested kriging model [44] (gray solid lines) and EM simulation at the design produced by the proposed model (—). The vertical lines denote the target operating frequencies: (a) $f_0 = 1.2$ GHz, $K_P = -2$ dB, (b) $f_0 = 1.5$ GHz, $K_P = -3$ dB, (c) $f_0 = 1.5$ GHz, $K_P = 0$ dB, (d) $f_0 = 1.7$ GHz, $K_P = -4$ dB.

surrogate and EM simulation model; the agreement between these two data sets is excellent. Similarly as for the previous example, both the nested kriging and the proposed modeling technique are significantly better than the surrogates constructed using conventional methods. Furthermore, the presented approach exhibits the predictive power better than the nested kriging for $K = 3$. For $K = 4$, the accuracy of both the nested kriging and the proposed surrogate are comparable but one needs to consider that the model domain volume is much larger for the proposed technique with $K = 4$ than for the nested kriging. Overall, the benefits are not as pronounced as for the transformer of Section III.A because dimensionality reduction for the coupler is limited (with respect to the original parameter space dimensionality of six).

Similarly as for the previous case, the eigenvalue analysis clearly indicate that the right choice of the parameter K is three. The normalized eigenvalues of the reference set for this problem are $\lambda_1 = 1.00$, $\lambda_2 = 0.12$, $\lambda_3 = 0.035$, $\lambda_4 = 0.0036$, $\lambda_5 = 0.0009$, $\lambda_6 = 0.0001$. Thus, the third eigenvalue is less than four percent of the first one, whereas the fourth one is an order of magnitude smaller than the third. Hence, involving another dimension ($K = 4$) would not bring meaningful information.

Verification of the design utility of the proposed modeling procedure was carried out the same way as in Section III.A, i.e., by optimizing the surrogate (here, obtained with $K = 3$ and $N = 400$) for several target operating frequencies and power split ratios. The results were compared to those obtained with the nested kriging model, cf. Fig. 9. It can be observed that that dimensionality reduction does not lead to design quality degradation. The geometry parameter values at the optimized designs can be found in Table 4.

TABLE 4. Application case studies: optimization of the rat-race coupler of Fig. 7.

Target operating conditions		Geometry parameter values [mm]					
f_0 [GHz]	K_P [dB]	l_1	l_2	l_3	d	w	w_1
1.2	–2	4.06	10.73	19.04	0.33	1.04	0.56
1.5	–3	3.89	10.74	16.12	0.30	0.98	0.48
1.5	0	4.34	11.21	15.98	0.22	0.72	0.72
1.7	–4	3.73	9.91	14.11	0.27	0.93	0.35

IV. CONCLUSION

This work discussed a new approach to computationally-efficient and accurate surrogate modelling of compact microwave components. Our methodology employs two major components: a recently proposed nested kriging framework, and spectral decomposition of the reference design set. The knowledge of the correlations between the figures of interest pertinent to the structure at hand and the reference points permits reduction of the surrogate model domain dimensionality as compared to the nested kriging. This leads to a further improvement of the model predictive power. The analytical formulation of the presented method includes procedures for convenient design of experiments (uniform data sampling), optimization of the surrogate model, as well as generation of a good initial design for a given target vector of performance specifications.

Our modelling technique has been validated using two miniaturized microstrip components, an impedance matching transformer described by fifteen geometry parameters, and a rat-race coupler described by six parameters. In both cases, the surrogates were rendered over broad ranges of parameters and operating conditions. Furthermore, comparisons with conventional modelling techniques (kriging and radial basis function interpolation, both over unconstrained domain) as well as the nested kriging have been included. The results demonstrate superiority of our approach in terms of

the surrogate model reliability across the considered training data sets of various sizes. The method of selecting the model domain dimensionality based on the eigenvalue analysis was discussed as well.

Finally, the paper presented applications of the models for design optimization (parameter tuning), as a way of demonstrating the design utility of the proposed technique. The conclusion from these experiments is that neither domain confinement nor dimensionality reduction have negative effects on the quality of the designs obtained using our approach.

ACKNOWLEDGMENT

The authors would like to thank Dassault Systemes, France, for making CST Microwave Studio available.

REFERENCES

[1] J. Ossorio, J. Vague, V. E. Boria, and M. Guglielmi, "Exploring the tuning range of channel filters for satellite applications using electromagnetic-based computer aided design tools," *IEEE Trans. Microw. Theory Techn.*, vol. 66, no. 2, pp. 717–725, Feb. 2018.

[2] P. Chen, B. M. Merrick, and T. J. Brazil, "Bayesian optimization for broadband high-efficiency power amplifier designs," *IEEE Trans. Microw. Theory Techn.*, vol. 63, no. 12, pp. 4263–4272, Dec. 2015.

[3] J. Zhang, F. Feng, W. Na, S. Yan, and Q. Zhang, "Parallel space-mapping based yield-driven EM optimization incorporating trust region algorithm and polynomial chaos expansion," *IEEE Access*, vol. 7, pp. 143673–143683, 2019.

[4] M. U. Memon, A. Salim, H. Jeong, and S. Lim, "Metamaterial inspired radio frequency-based touchpad sensor system," *IEEE Trans. Instrum. Meas.*, vol. 69, no. 4, pp. 1344–1352, Apr. 2020.

[5] C.-H. Tseng and C.-L. Chang, "A rigorous design methodology for compact planar branch-line and rat-race couplers with asymmetrical T-structures," *IEEE Trans. Microw. Theory Techn.*, vol. 60, no. 7, pp. 2085–2092, Jul. 2012.

[6] S. Koziel and P. Kurgan, "Compact cell topology selection for size-reduction-oriented design of microstrip rat-race couplers," *Int. J. RF Microw. Comput.-Aided Eng.*, vol. 28, no. 5, Jun. 2018, Art. no. e21261.

[7] Y. Zheng and W. Sheng, "Compact lumped-element LTCC bandpass filter for low-loss VHF-band applications," *IEEE Microw. Wireless Compon. Lett.*, vol. 27, no. 12, pp. 1074–1076, Dec. 2017.

[8] J.-X. Chen, Y.-L. Li, W. Qin, Y.-J. Yang, and Z.-H. Bao, "Compact multilayer bandpass filter with wide stopband using selective feeding scheme," *IEEE Trans. Circuits Syst. II, Exp. Briefs*, vol. 65, no. 8, pp. 1009–1013, Aug. 2018.

[9] S. Koziel and A. Pietrenko-Dabrowska, "Rapid optimization of compact microwave passives using kriging surrogates and iterative correction," *IEEE Access*, vol. 8, pp. 53587–53594, 2020.

[10] A. Toktas, D. Ustun, and M. Tekbas, "Multi-objective design of multi-layer radar absorber using surrogate-based optimization," *IEEE Trans. Microw. Theory Techn.*, vol. 67, no. 8, pp. 3318–3329, Aug. 2019.

[11] B. Liu, H. Yang, and M. J. Lancaster, "Global optimization of microwave filters based on a surrogate model-assisted evolutionary algorithm," *IEEE Trans. Microw. Theory Techn.*, vol. 65, no. 6, pp. 1976–1985, Jun. 2017.

[12] X.-K. Gao, H. M. Lee, and S.-P. Gao, "A robust parameter design of wide band DGS filter for common-mode noise mitigation in high-speed electronics," *IEEE Trans. Electromagn. Compat.*, vol. 59, no. 6, pp. 1735–1740, Dec. 2017.

[13] S. Koziel and J. W. Bandler, "Rapid yield estimation and optimization of microwave structures exploiting feature-based statistical analysis," *IEEE Trans. Microw. Theory Techn.*, vol. 63, no. 1, pp. 107–114, Jan. 2015.

[14] M. Sengupta, S. Saxena, L. Daldoss, G. Kramer, S. Minehane, and J. Cheng, "Application-specific worst case corners using response surfaces and statistical models," *IEEE Trans. Comput.-Aided Design Integr. Circuits Syst.*, vol. 24, no. 9, pp. 1372–1380, Sep. 2005.

[15] A. Pietrenko-Dabrowska and S. Koziel, "Computationally-efficient design optimisation of antennas by accelerated gradient search with sensitivity and design change monitoring," *IET Microw., Antennas Propag.*, vol. 14, no. 2, pp. 165–170, Feb. 2020.

[16] S. Koziel and A. Pietrenko-Dabrowska, "Expedited optimization of antenna input characteristics with adaptive Broyden updates," *Eng. Comp.*, vol. 37, no. 3, pp. 851–862, 2019, doi: 10.1108/ec-01-2019-0023.

[17] J. E. Rayas-Sanchez, "Power in simplicity with ASM: Tracing the aggressive space mapping algorithm over two decades of development and engineering applications," *IEEE Microw. Mag.*, vol. 17, no. 4, pp. 64–76, Apr. 2016.

[18] S. Koziel and L. Leifsson, *Simulation-Driven Design By Knowledge-Based Response Correction Techniques*. New York, NY, USA: Springer, 2016.

[19] A. I. J. Forrester and A. J. Keane, "Recent advances in surrogate-based optimization," *Prog. Aerosp. Sci.*, vol. 45, nos. 1–3, pp. 50–79, Jan. 2009.

[20] C. Zhang, F. Feng, V.-M.-R. Gongal-Reddy, Q. J. Zhang, and J. W. Bandler, "Cognition-driven formulation of space mapping for equal-ripple optimization of microwave filters," *IEEE Trans. Microw. Theory Techn.*, vol. 63, no. 7, pp. 2154–2165, Jul. 2015.

[21] F. Feng, J. Zhang, W. Zhang, Z. Zhao, J. Jin, and Q.-J. Zhang, "Coarse- and fine-mesh space mapping for EM optimization incorporating mesh deformation," *IEEE Microw. Wireless Compon. Lett.*, vol. 29, no. 8, pp. 510–512, Aug. 2019.

[22] S. Koziel and S. D. Unnsteinsson, "Expedited design closure of antennas by means of trust-region-based adaptive response scaling," *IEEE Antennas Wireless Propag. Lett.*, vol. 17, no. 6, pp. 1099–1103, Jun. 2018.

[23] S. Koziel, J. W. Bandler, and K. Madsen, "Space mapping with adaptive response correction for microwave design optimization," *IEEE Trans. Microw. Theory Techn.*, vol. 57, no. 2, pp. 478–486, Feb. 2009.

[24] S. Koziel, Q. S. Cheng, J. W. Bandler, and S. Ogurtsov, "Rapid electromagnetic-based microwave design optimisation exploiting shape-preserving response prediction and adjoint sensitivities," *IET Microw., Antennas Propag.*, vol. 8, no. 10, pp. 775–781, Jul. 2014.

[25] S. Koziel and S. Ogurtsov, *Antenna Design By Simulation-Driven Optimization* (Surrogate-Based Approach). New York, NY, USA: Springer, 2014.

[26] J. C. Cervantes-González, J. E. Rayas-Sánchez, C. A. López, J. R. Camacho-Pérez, Z. Brito-Brito, and J. L. Chávez-Hurtado, "Space mapping optimization of handset antennas considering EM effects of mobile phone components and human body," *Int. J. RF Microw. Comput.-Aided Eng.*, vol. 26, no. 2, pp. 121–128, Feb. 2016.

[27] S. Koziel, "Fast simulation-driven antenna design using response-feature surrogates," *Int. J. RF Microw. Comput.-Aided Eng.*, vol. 25, no. 5, pp. 394–402, Jun. 2015.

[28] H. M. Torun and M. Swaminathan, "High-dimensional global optimization method for high-frequency electronic design," *IEEE Trans. Microw. Theory Techn.*, vol. 67, no. 6, pp. 2128–2142, Jun. 2019.

[29] D. R. Jones, M. Schonlau, and W. J. Welch, "Efficient global optimization of expensive black-box functions," *J. Global Optim.*, vol. 13, no. 4, pp. 455–492, 1998.

[30] A. M. Alzahed, S. M. Mikki, and Y. M. M. Antar, "Nonlinear mutual coupling compensation operator design using a novel electromagnetic machine learning paradigm," *IEEE Antennas Wireless Propag. Lett.*, vol. 18, no. 5, pp. 861–865, May 2019.

[31] X. Wang, G. G. Wang, B. Song, P. Wang, and Y. Wang, "A novel evolutionary sampling assisted optimization method for high-dimensional expensive problems," *IEEE Trans. Evol. Comput.*, vol. 23, no. 5, pp. 815–827, Oct. 2019.

[32] H. Wang, Y. Jin, and J. Doherty, "Committee-based active learning for surrogate-assisted particle swarm optimization of expensive problems," *IEEE Trans. Cybern.*, vol. 47, no. 9, pp. 2664–2677, Sep. 2017.

[33] J. van der Herten, I. Couckuyt, D. Deschrijver, and T. Dhaene, "Adaptive classification under computational budget constraints using sequential data gathering," *Adv. Eng. Softw.*, vol. 99, pp. 137–146, Sep. 2016.

[34] S. Marelli and B. Sudret, "UQLab: A framework for uncertainty quantification in MATLAB," in *Proc. 2nd Int. Conf. Vulnerability Risk Anal. Manage. (ICVRAM)*. Liverpool, U.K.: Univ. Liverpool, Jul. 2014, pp. 2554–2563.

[35] J. L. Chavez-Hurtado and J. E. Rayas-Sanchez, "Polynomial-based surrogate modeling of RF and microwave circuits in frequency domain exploiting the multinomial theorem," *IEEE Trans. Microw. Theory Techn.*, vol. 64, no. 12, pp. 4371–4381, Dec. 2016.

[36] W. Liu, W. Na, L. Zhu, J. Ma, and Q.-J. Zhang, "A Wiener-type dynamic neural network approach to the modeling of nonlinear microwave devices," *IEEE Trans. Microw. Theory Techn.*, vol. 65, no. 6, pp. 2043–2062, Jun. 2017.

[37] T. W. Simpson, J. D. Poplinski, P. N. Koch, and J. K. Allen, "Metamodels for computer-based engineering design: Survey and recommendations," *Eng. Comput.*, vol. 17, no. 2, pp. 129–150, Jul. 2001.
[38] D. I. L. de Villiers, I. Couckuyt, and T. Dhaene, "Multi-objective optimization of reflector antennas using kriging and probability of improvement," in *Proc. IEEE Int. Symp. Antennas Propag.*, San Diego, CA, USA, Jul. 2017, pp. 985–986.
[39] J. Cai, J. King, C. Yu, J. Liu, and L. Sun, "Support vector regression-based behavioral modeling technique for RF power transistors," *IEEE Microw. Wireless Compon. Lett.*, vol. 28, no. 5, pp. 428–430, May 2018.
[40] J. Cai, C. Yu, L. Sun, S. Chen, and J. B. King, "Dynamic behavioral modeling of RF power amplifier based on time-delay support vector regression," *IEEE Trans. Microw. Theory Techn.*, vol. 67, no. 2, pp. 533–543, Feb. 2019.
[41] J. Zhang, C. Zhang, F. Feng, W. Zhang, J. Ma, and Q.-J. Zhang, "Polynomial chaos-based approach to yield-driven EM optimization," *IEEE Trans. Microw. Theory Techn.*, vol. 66, no. 7, pp. 3186–3199, Jul. 2018.
[42] A. Petrocchi, A. Kaintura, G. Avolio, D. Spina, T. Dhaene, A. Raffo, and D. M. M.-P. Schreurs, "Measurement uncertainty propagation in transistor model parameters via polynomial chaos expansion," *IEEE Microw. Wireless Compon. Lett.*, vol. 27, no. 6, pp. 572–574, Jun. 2017.
[43] A. K. Prasad and S. Roy, "Accurate reduced dimensional polynomial chaos for efficient uncertainty quantification of microwave/RF networks," *IEEE Trans. Microw. Theory Techn.*, vol. 65, no. 10, pp. 3697–3708, Apr. 2017.
[44] L. Leifsson, X. Du, and S. Koziel, "Efficient yield estimation of multiband patch antennas by polynomial chaos-based kriging," *Int. J. Numer. Model., Electron. Netw., Devices Fields*, Jan. 2020, Art. no. e2722.
[45] A. C. Yücel, H. Bağcı, and E. Michielssen, "An ME-PC enhanced HDMR method for efficient statistical analysis of multiconductor transmission line networks," *IEEE Trans. Compon., Packag., Manuf. Technol.*, vol. 5, no. 5, pp. 685–696, May 2015.
[46] X. Li, "Finding deterministic solution from underdetermined equation: Large-scale performance variability modeling of analog/RF circuits," *IEEE Trans. Comput.-Aided Design Integr. Circuits Syst.*, vol. 29, no. 11, pp. 1661–1668, Nov. 2010.
[47] M. Kennedy, "Predicting the output from a complex computer code when fast approximations are available," *Biometrika*, vol. 87, no. 1, pp. 1–13, Mar. 2000.
[48] J. P. Jacobs and S. Koziel, "Two-stage framework for efficient Gaussian process modeling of antenna input characteristics," *IEEE Trans. Antennas Propag.*, vol. 62, no. 2, pp. 706–713, Feb. 2014.
[49] F. Wang, P. Cachecho, W. Zhang, S. Sun, X. Li, R. Kanj, and C. Gu, "Bayesian model fusion: Large-scale performance modeling of analog and mixed-signal circuits by reusing early-stage data," *IEEE Trans. Comput.-Aided Design Integr. Circuits Syst.*, vol. 35, no. 8, pp. 1255–1268, Aug. 2016.
[50] S. Koziel, "Low-cost data-driven surrogate modeling of antenna structures by constrained sampling," *IEEE Antennas Wireless Propag. Lett.*, vol. 16, pp. 461–464, 2017.
[51] S. Koziel and A. T. Sigurdsson, "Triangulation-based constrained surrogate modeling of antennas," *IEEE Trans. Antennas Propag.*, vol. 66, no. 8, pp. 4170–4179, Aug. 2018.
[52] S. Koziel and A. Pietrenko-Dabrowska, "Performance-based nested surrogate modeling of antenna input characteristics," *IEEE Trans. Antennas Propag.*, vol. 67, no. 5, pp. 2904–2912, May 2019.
[53] S. Koziel and A. Pietrenko-Dabrowska, "Reliable data-driven modeling of high-frequency structures by means of nested kriging with enhanced design of experiments," *Eng. Comput.*, vol. 36, no. 7, pp. 2293–2308, 2019.
[54] I. T. Jolliffe, *Principal Component Analysis*, 2nd ed. New York, NY, USA: Springer, 2002.
[55] D. Bau, III, and L. N. Trefethen, *Numerical Linear Algebra*. Philadelphia, PA, USA: SIAM, 1997.
[56] N. V. Queipo, R. T. Haftka, W. Shyy, T. Goel, R. Vaidynathan, and P. K. Tucker, "Surrogate based analysis and optimization," *Prog. Aerosp. Sci.*, vol. 41, no. 1, pp. 1–28, 2005.
[57] B. Beachkofski and R. Grandhi, "Improved distributed hypercube sampling," in *Proc. Amer. Inst. Aeronaut. Astronaut.*, 2002, p. 1274.
[58] A. Pietrenko-Dabrowska and S. Koziel, "Accelerated multiobjective design of miniaturized microwave components by means of nested kriging surrogates," *Int. J. RF Microw. Comput.-Aided Eng.*, vol. 30, no. 4, Apr. 2020, Art. no. e22124.
[59] S. Koziel and A. T. Sigurdsson, "Performance-driven modeling of compact couplers in restricted domains," *Int. J. RF Microw. Comput.-Aided Eng.*, vol. 28, no. 6, Aug. 2018, Art. no. e21296.

SLAWOMIR KOZIEL (Senior Member, IEEE) received the M.Sc. and Ph.D. degrees in electronic engineering from the Gdansk University of Technology, Poland, in 1995 and 2000, respectively, and the M.Sc. degrees in theoretical physics and mathematics and the Ph.D. degree in mathematics from the University of Gdansk, Poland, in 2000, 2002, and 2003, respectively. He is currently a Professor with the Department of Engineering, Reykjavik University, Iceland. His research interests include CAD and modeling of microwave and antenna structures, simulation-driven design, surrogate-based optimization, space mapping, circuit theory, analog signal processing, evolutionary computation, and numerical analysis.

ANNA PIETRENKO-DABROWSKA (Senior Member, IEEE) received the M.Sc. and Ph.D. degrees in electronic engineering from the Gdansk University of Technology, Poland, in 1998 and 2007, respectively. She is currently an Associate Professor with the Gdansk University of Technology. Her research interests include simulation-driven design, design optimization, control theory, modeling of microwave and antenna structures, and numerical analysis.

MU'ATH AL-HASAN (Senior Member, IEEE) received the B.Sc. degree in electrical engineering from the Jordan University of Science and Technology, Jordan, in 2005, the M.Sc. degree in wireless communications from Yarmouk University, Jordan, in 2008, and the Ph.D. degree in telecommunication engineering from the Institut National de la Recherche Scientifique (INRS), Université du Québec, Canada, in 2015. From 2013 to 2014, he was with Planets Inc., San Francisco, CA, USA. In May 2015, he joined Concordia University, Canada, as a Postdoctoral Fellowship. He is currently an Assistant Professor with Al Ain University, United Arab Emirates. His current research interests include antenna design at millimeter-wave and terahertz, channel measurements in multiple-input and multiple-output (MIMO) systems, machine learning, and artificial intelligence in antenna design.